Int. J. Solids Structures, Vol. 11, pp. 1301–1314. Pergamon Press 1975. Printed in Great Britain

BIFURCATION OF A RUNNING CRACK IN ANTIPLANE STRAIN

J. D. ACHENBACH

Department of Civil Engineering, The Technological Institute, Northwestern University, Evanston, IL 60201, U.S.A.

(*Received* 22 *January* 1975; *revised* 11 *April* 1975)

Abstract—An elastodynamic explanation of running crack bifurcation is explored. The geometry is a semi-infinite body in a state of antiplane strain, which contains a two-dimensional edge crack. It is assumed that a quasi-static increase of the external loads gives rise to rapid crack propagation at time $t = 0$, with an arbitrary and time-varying speed, but in the plane of the crack. A short time later the crack is assumed to bifurcate at angles $-\kappa\pi$ and $+\kappa\pi$, and with velocities v. The elastodynamic intensity factors are computed, and the balance of rates of energies is employed to discuss the conditions for bifurcation.

1. FORMULATION OF THE PROBLEM

Once the propagation of a crack has started, the primary crack often bifurcates into two or more branches, each of which may propagate over a short distance, and then again split into two or more new branches. Crack bifurcation occurs in a variety of materials, and under different external conditions. The phenomenon is, however, particularly frequent for essentially brittle fracture, when the speed of crack propagation becomes relatively large.

It requires sophisticated high-speed photographical equipment to take a sequence of photographs showing the evolution of the pattern of bifurcating cracks. The techniques which are available for this purpose have been developed and described by Schardin[1] and Kerkhof[2, p. 108]. In both[1] and[2] a number of shadow photographs of bifurcating cracks are shown, and numerical information on speeds of crack propagation is presented. A paper by Kalthof[3] dealing with bifurcation of a primary edge crack in a stretched glass plate, includes a sequence of shadow photographs at a framing rate of 4 μs, which is particularly illustrative of the first bifurcation of the primary crack.

The amount of analytical work dealing with crack branching under an arbitrary angle with the primary crack is rather limited. For antiplane strain, elastostatic analyses were presented by Sih[4] and Smith[5]. The elastostatic in-plane problem of a single branch emanating from a primary crack has recently been treated by Hussain, Pu and Underwood[6], and Palaniswamy and Knauss[7]. In addition there have been proposals to determine the conditions for crack branching from the stress field around the unbranched crack. Frequently discussed among these is a recent criterion due to Sih[8], which is based on the distribution of strain energy around the crack tip of the primary crack.

The analytical works cited above are elastostatic in nature. Experimental observations of the magnitude of the speed of crack propagation at branching, see[1, 2], suggest, however, that elastodynamic effects play a significant role. Another indication of the importance of elastodynamic effects is found in the observation that for a crack propagating in its own plane, under the influence of uniaxial tension, the maximum values of elastodynamic stresses move out of the plane of crack propagation when the crack propagation velocity exceeds a certain critical value, see[9–12].

Bifurcation of a running crack is an instability phenomenon. A necessary condition for bifurcation can be determined by comparing states prior to branching and after branching has taken place. The comparison requires expressions for the elastodynamic fields near the tips of the branches. For symmetric branching in antiplane strain the near-tip fields are analyzed in this paper by extending the analytical work of[13]. The necessary condition for bifurcation of a running crack is subsequently established on the basis of the balance of rates of energies.

The particular problem considered here concerns the two-dimensional geometry of an edge crack of depth a in a semi-infinite elastic solid. In a cartesian coordinate system (x, y, z) the position of the crack tip is defined by $x = a$, and the z-axis is parallel to the edges of the crack, as shown in Fig. 1. The solid is subjected to a distribution of equal and opposite concentrated forces

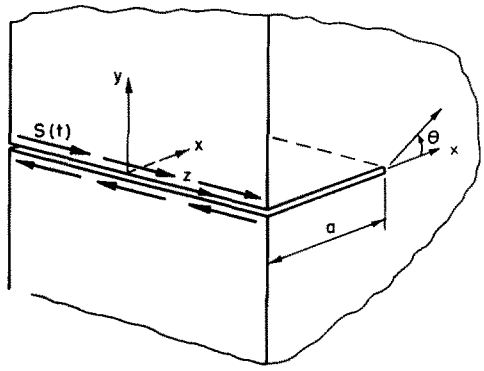

Fig. 1. Tearing of an edge crack.

in the z-direction, applied at $x = 0$ and $y = \pm\epsilon$, where ϵ is very small. These antiplane shear forces of magnitude $Z = S(t)$ force units per unit length give rise to deformations in antiplane strain. It is assumed that the fields of stress and deformation generated by $S(t)$ are *elastostatic* in nature. The stress component τ_{yz} is of the general form

$$\tau_{yz} = g(x, y)\, S(t). \tag{1.1}$$

Let us now suppose that at time $t = 0$ a rapid Mode III tearing process starts, and that the crack begins to propagate, initially in its own plane, so that the position of the crack tip is defined by $x = a + X(t)$. The process of crack propagation implies that tractions $\tau_{yz} = g(x, 0)\, S(t)$ are removed from $a < x < a + X(t)$, as follows from eqn (1.1). It is assumed that the fields generated by the propagation of the crack are *elastodynamic* in nature.

In a two-dimensional geometry antiplane displacements $w(x, y, t)$ are governed by $\nabla^2 w = (1/c^2)\partial^2 w/\partial t^2$, where ∇^2 is the Laplacian, and c is the velocity of transverse waves, $c = (\mu/\rho)^{1/2}$. Here μ and ρ are the shear modulus and the mass density, respectively. We consider the case that the speed of crack propagation is smaller than the velocity of transverse waves, i.e.

$$\frac{dX}{dt} < c,\ c = (\mu/\rho)^{1/2}. \tag{1.2}$$

The propagation of a crack in its own plane has been analyzed in detail, see e.g. [14], at least for small times. Some pertinent results will be briefly reviewed in Section 2. In this paper we wish, however, to consider the case that subsequent to propagation in its own plane in the time interval $0 < t < t_{bf}$, the crack bifurcates symmetrically under angles $\pm\kappa\pi$ from the points defined by $x = a + X(t_{bf})$. The elasto-dynamic fields generated by the removal of tractions from the crack branches and the subsequent application of the balance of rates of energies are the principal topics of analysis of the present paper.

2. RAPID CRACK PROPAGATION IN THE PLANE OF THE CRACK

It is well-known that the stress components and the particle velocity are singular at a moving crack tip. In terms of a system of cylindrical coordinates (R, φ, z) which is attached to the moving crack tip, see Fig. 2, the singular parts of the shear stress $\tau_{\varphi z}$ and the particle velocity $\dot{w}$ are of the forms

$$\tau_{\varphi z} = T_{\varphi z}(\varphi, t) R^{-1/2}, \quad \text{and} \quad \dot{w} = \dot{W}(\varphi, t) R^{-1/2}. \tag{2.1a, b}$$

The functions $T_{\varphi z}$ and $\dot{W}$, which generally depend on time, the angle φ, and the geometrical and material parameters, are termed the stress-intensity function and the velocity-intensity function, respectively.

For antiplane strain, the elastodynamic fields generated in the plane of the crack by the removal of tractions of the type given by eqn (1.1) from the newly formed fracture surface were investigated in some detail in [14, p. 34]. The following result was obtained

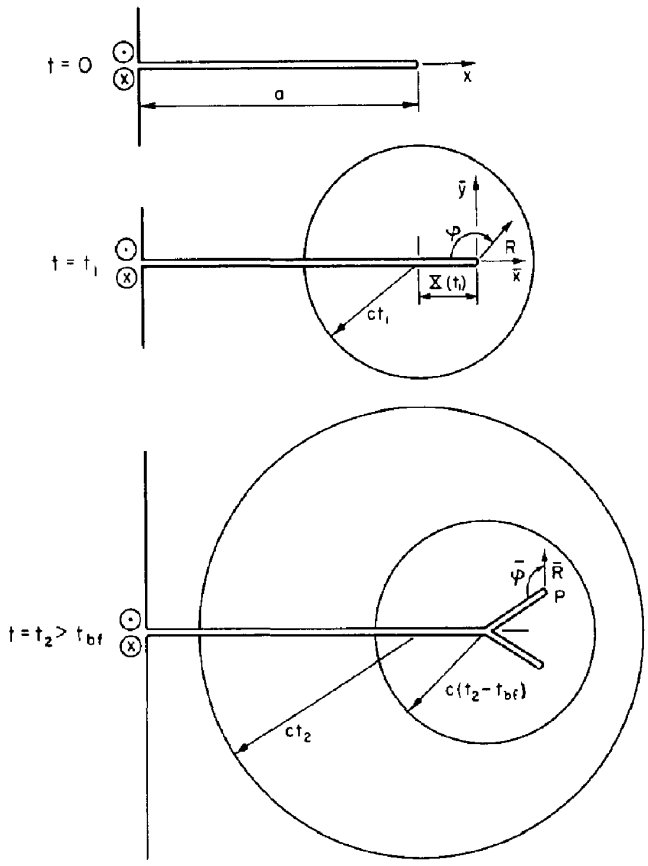

Fig. 2. Rapid propagation and bifurcation in antiplane strain of an edge crack.

$$T_{\varphi z}(\pi, t) = \frac{1}{\pi}(1-\alpha)^{1/2} I(t), \tag{2.2}$$

where

$$\alpha = \frac{1}{c}\frac{dX}{dt}, \tag{2.3}$$

and

$$I(t) = S(t)\int_0^{X(t)-a} \frac{g(v,0)\,dv}{[X(t)-a-v]^{1/2}}. \tag{2.4}$$

Also

$$\dot{W}(0,t) = \frac{c}{\pi\mu}(1+\alpha)^{-1/2}\alpha I(t). \tag{2.5}$$

These expressions are valid for $0 \le t \le 2a/c$.

For essentially brittle fracture the balance of rates of energies provides a necessary condition for crack propagation. The balance of rates of energies states

$$F = 2\gamma_F \frac{dX}{dt} \tag{2.6}$$

Where F is the energy flux into the crack tip, and γ_F is the specific surface energy, which is assumed to be constant-valued. It follows from the results of Achenbach [14] and Freund [15] that the flux of energy into a propagating crack tip in Mode III fracture can be expressed in the form

$$F = \pi T_{\varphi z}(\pi, t)\, \dot{W}(0,t). \tag{2.7}$$

Substituting eqns (2.2) and (2.5) into (2.7) and (2.6), we obtain

$$\left(\frac{1-\alpha}{1+\alpha}\right)^{1/2}\alpha = \frac{2\pi\gamma_F\mu}{[I(t)]^2}\alpha. \tag{2.8}$$

This balance of rates of energies yields not only the critical magnitude of the externally applied tractions, but also a nonlinear ordinary differential equation for $X(t)$. If the left and right-hand sides of eqn (2.8) are plotted vs α, the term $[2\pi\gamma_F\mu/I^2(t)]\alpha$ is a straight line through the origin, whose slope decreases as $I(t)$ increases. The necessary condition for fracture is satisfied when the slope is smaller than the slope of $(1-\alpha)^{1/2}\alpha/(1+\alpha)^{1/2}$ at $\alpha = 0$, i.e. when

$$2\pi\gamma_F\mu \leq [I(t)]^2. \tag{2.9}$$

Thus, eqn (2.9) provides a necessary condition for initiation of fracture. For $I(t) > (2\pi\gamma_F\mu)^{1/2}$ the dimensionless speed of crack propagation α can be computed from eqn (2.8).

For the problem described in Section 1, and illustrated in Fig. 1, the stress in the plane of the crack prior to fracture can be computed. Referring to eqn (1.1), the function $g(x, 0)$ in the immediate vicinity of the crack tip is of the form

$$g(x,0) = \frac{1}{\pi}\left(\frac{2}{a}\right)^{1/2}\left(\frac{1}{x-a}\right)^{1/2} + 0[(x-a)^{1/2}]. \tag{2.10}$$

Substituting eqn (2.10) into the integral $I(t)$, eqn (2.4), we obtain

$$I = \left(\frac{2}{a}\right)^{1/2} S(t) + \text{higher order terms}. \tag{2.11}$$

The critical magnitude of the external load $S(t)$ immediately follows from (2.9) and (2.11) as

$$S_{cr} = (\pi\mu\gamma_F a)^{1/2}. \tag{2.12}$$

At the very beginning of the fracture process, when $X(t) \ll a$, the higher order terms in eqn (2.11) can be neglected. The dimensionless speed of crack propagation can then be computed from eqns (2.8) and (2.11) as

$$\alpha = \frac{1}{c}\frac{dX}{dt} = \frac{[S(t)/S_{cr}]^4 - 1}{[S(t)/S_{cr}]^4 + 1}. \tag{2.13}$$

There will be an instantaneous speed of crack propagation if $S(t)$ exceeds S_{cr} at the instant that fracture starts.

It is of interest to compute the magnitude of dX/dt for a few values of $S(t)/S_{cr}$. We find $S(t)/S_{cr} = 1$: $dX/dt = 0$; $S(t)/S_{cr} = 1{\cdot}1$: $dX/dt = 0{\cdot}188c$; $S(t)/S_{cr} = 1{\cdot}2$: $dX/dt = 0{\cdot}35c$. Evidently the speed of crack propagation becomes already comparable to the speed of transverse waves when the external loads are increased by only about ten percent.

In the foregoing we have obtained the singular part of the stress in the plane of the propagating crack, i.e. $T_{\varphi z}(\pi, t)$. The angular variation of the stress singularity near the propagating crack tip can be analyzed in a very simple manner by a method which was employed in static elasticity by Williams[16]. For elastodynamic problems this method was explored in considerable detail in[12], where it is shown that in the immediate vicinity of the moving crack tip the stress $\tau_{\varphi z}$ is of the form

$$\tau_{\varphi z} = \frac{1}{2}T(t)(1-\alpha^2)^{1/2}\Phi_\tau(\alpha, \varphi)R^{-1/2} \tag{2.14}$$

where α is defined by eqn (2.3). For $0 \leq \varphi \leq \pi$, we have

$$\Phi_\tau = (1-\alpha^2)^{-1/2}\Phi_1 \sin\phi - \Phi_2\cos\phi \tag{2.15}$$

where

$$\Phi_1 = \left[\frac{(1-\alpha^2\sin^2\varphi)^{1/2}+\cos\varphi}{1-\alpha^2\sin^2\varphi}\right]^{1/2} \tag{2.16}$$

$$\Phi_2 = \left[\frac{(1-\alpha^2\sin^2\varphi)^{1/2}-\cos\varphi}{1-\alpha^2\sin^2\varphi}\right]^{1/2}. \tag{2.17}$$

For various values of α, the function $\Phi_\tau(\alpha, \varphi)$ is plotted vs φ in Fig. 5 of [13]. The plot shows that the maximum value of Φ_τ moves out of the plane of crack propagation, $\varphi = \pi$, as α reaches a value slightly smaller than 0·6. Comparing eqns (2.14), (2.1) and (2.2) it is concluded that the intensity function $T_{\varphi z}$ is

$$T_{\varphi z} = \frac{1}{\pi}\frac{1}{\sqrt{2}}(1-\alpha)^{1/2} I(t)\Phi_\tau(\alpha, \varphi), \tag{2.18}$$

where $I(t)$ is defined by eqn (2.4).

The bifurcation of a running crack may be thought of as consisting of arrest of propagation in the plane of the crack, immediately followed by initiation of the two branches. When the propagation in the plane of the crack stops at $t = t_{bf}$, a cylindrical wave is generated. The position of the wavefront of this wave at time $t > t_{bf}$ is indicated in Fig. 2. By setting $dX/dt = 0$, the singularity at $x = a + X(t_{bf})$ compatible with crack arrest follows from eqn (2.18) as

$$\tau_{\varphi z} = AH(t - t_{bf}) \sin(\varphi/2) R^{-1/2} \tag{2.19}$$

where

$$A = \frac{1}{\pi} I(t_{bf}). \tag{2.20}$$

In the immediately following process of symmetric bifurcation at velocities v, where $v/c < 1$, the stress given by eqn (2.19) is removed from the branches which are defined by $R < vt$, $\varphi = \pi \pm \kappa\pi$.

A particular problem of crack bifurcation is examined in the next section, and we will return to the discussion of bifurcation of a running crack in Section 4.

3. ANALYSIS OF INSTANTANEOUS CRACK BIFURCATION

In a stationary system of polar coordinates, r and θ, two-dimensional antiplane wave motions are governed by

$$\frac{1}{r}\frac{\partial}{\partial r}\left(r\frac{\partial w}{\partial r}\right) + \frac{1}{r^2}\frac{\partial^2 w}{\partial \theta^2} = \frac{1}{c^2}\frac{\partial^2 w}{\partial t^2} \tag{3.1}$$

where $w(r, \theta, t)$ is the out-of-plane displacement, and c is the velocity of transverse waves. The relevant shear stresses are

$$\tau_{rz} = \mu \partial w/\partial r, \quad \tau_{\theta z} = (\mu/r)\partial w/\partial \theta. \tag{3.2a, b}$$

As a preliminary to the analysis of branching of a running crack we analyze in this section the elastodynamic fields which are generated when two branches emanate symmetrically from the tip of a stationary semi-infinite crack, upon the sudden application of equal and opposite uniform antiplane shear tractions to the two semi-infinite surfaces of the crack. The shear tractions produce two plane waves, and a diffracted cylindrical wave with center at the original crack tip. It is assumed that the semi-infinite crack bifurcates at the instant that the shear tractions are applied, and that bifurcation takes place at angles $\pm\kappa\pi$, and with constant velocities v, where $v/c < 1$. At time $t > 0$, the crack tips are located at points C and D, which are defined by $r = vt$, $\theta = -\kappa\pi$ and $r = vt$, $\theta = \kappa\pi$, respectively. The pattern of wavefronts and the positions of the crack tips are shown in Fig. 3. Note that L, M and N all denote the original crack tip, but at different sides of the fracture surface.

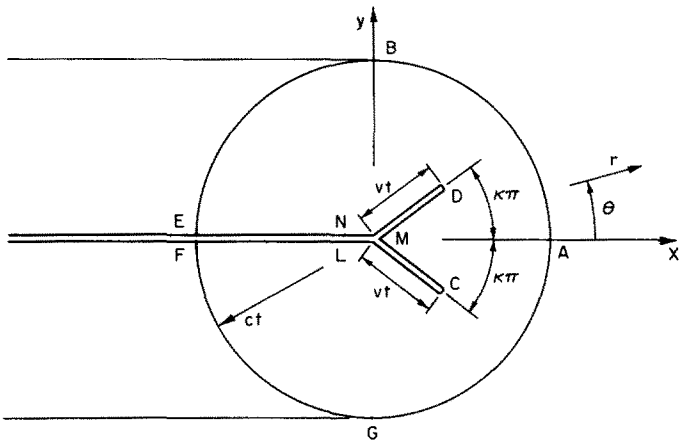

Fig. 3. Pattern of wave fronts and positions of crack tips for instantaneous bifurcation of a semi-infinite crack.

The problem described above is governed by eqn (3.1). The conditions on the physical boundaries are

$$\theta = \pm\pi, \quad r > 0: \quad \tau_{\theta z} = \tau_0 H(t) \tag{3.3}$$

$$\theta = \pm\kappa\pi, \quad 0 < r < vt: \quad \tau_{\theta z} = 0 \tag{3.4}$$

where τ_0 is the magnitude of the uniform distribution of shear tractions. The shear tractions at $\theta = \pm\pi$ generate plane waves, with constant particle velocities of magnitudes $\pm c\tau_0/\mu$. Along the segments BE and FG, see Fig. 3, the particle velocities then are

$$\frac{\pi}{2} < \theta \leq \pi, \quad r = ct: \quad \dot{w} = c\tau_0/\mu \tag{3.5}$$

$$-\pi \leq \theta \leq -\frac{\pi}{2}, \quad r = ct: \quad \dot{w} = -c\tau_0/\mu. \tag{3.6}$$

The material is undisturbed ahead of the segment BG, and thus

$$-\frac{\pi}{2} < \theta < \frac{\pi}{2}, \quad r = ct: \quad \dot{w} = 0. \tag{3.7}$$

Equations (3.3)–(3.7) can be considered as boundary conditions on $w(r, \theta, t)$ for the region of the cylindrical wave. It is evident from these conditions that the displacement field is antisymmetric with respect to $\theta = 0$, which implies that w, and thus $\dot{w}$ vanishes as $\theta = 0$:

$$\theta = 0, \quad 0 < r < ct: \quad \dot{w} = 0. \tag{3.8}$$

It then suffices to consider only the region $0 \leq \theta \leq \pi$, $0 < r \leq ct$.

Let us consider the particle velocity as the dependent variable. For $t > 0$ it then follows from eqns (3.3) and (3.4) that

$$\theta = \pi, \quad r > 0: \quad \frac{\partial \dot{w}}{\partial \theta} = 0 \tag{3.9}$$

$$\theta = \kappa\pi, \quad 0 < r < vt: \quad \frac{\partial \dot{w}}{\partial \theta} = 0. \tag{3.10}$$

Equations (3.5) and (3.7)–(3.10) are the conditions on the particle velocity $\dot{w}$, on the boundaries of the region $0 < r < ct$, $0 \leq \theta \leq \pi$. These conditions suggest that the particle velocity $\dot{w}$ is self-similar. The property of self-similarity implies that $\dot{w}$ depends on r/t and θ, rather than on θ

and r and t separately. As discussed in [17, p. 154] and [13] it is then convenient to introduce the new variable $s = r/t$, whereupon the equation for $\dot{w}(s, \theta)$ follows from eqn (3.1) as

$$s^2\left(1-\frac{s^2}{c^2}\right)\frac{\partial^2\dot{w}}{\partial s^2}+s\left(1-\frac{2s^2}{c^2}\right)\frac{\partial\dot{w}}{\partial s}+\frac{\partial^2\dot{w}}{\partial\theta^2}=0. \tag{3.11}$$

For $s < c$, Chaplygin's transformation $\beta = \cosh^{-1}(c/s)$, reduces eqn (3.11) to Laplace's equation

$$\frac{\partial^2\dot{w}}{\partial\beta^2}+\frac{\partial^2\dot{w}}{\partial\theta^2}=0, \quad \beta=\cosh^{-1}(c/s). \tag{3.12a, b}$$

The real transformation given by eqn (3.12b) maps the interior of the domain $0 \le \theta \le \pi$, $s < c$ into a semi-infinite strip in the $\theta - \beta$ plane containing a slit. The domain in the $\theta - \beta$ plane is shown in Fig. 4, where the boundary conditions corresponding to eqns (3.5)–(3.10) are also indicated.

In the $\theta - \beta$ plane the harmonic function $\dot{w}$ can be taken as the real part of an analytic function $G(\gamma)$

$$\dot{w} = Re\, G(\gamma), \quad \gamma = \beta + i\theta, \tag{3.13a,b}$$

where $G(\gamma)$ can formally be obtained by conformal mapping techniques. The domain in the γ-plane can be related to the upper half of the ζ-plane by means of a Schwarz–Christoffel transformation

$$\gamma = \omega(\zeta), \quad \zeta = \xi + i\eta. \tag{3.14, b}$$

An appropriate transformation is

$$\omega(\zeta) = C_1\int_1^{\zeta}\frac{u\,du}{(u+\xi_M)(u-\xi_N)(1-u^2)^{1/2}}+C_2. \tag{3.15}$$

Here C_1 and C_2 are complex constants. The ζ-plane is shown in Fig. 5. Eqn (3.15) implies that the points A and E are mapped at $\zeta = -1$ and $\zeta = +1$, respectively, while the point D is mapped into the origin $\zeta = 0$.

Equation (3.15) may be integrated to yield

$$\begin{aligned}\omega(\zeta) = &-\frac{\xi_M}{\xi_M+\xi_N}\frac{C_1}{(1-\xi_M^2)^{1/2}}\{\ln[(1-\xi_M^2)^{1/2}(1-\zeta^2)^{1/2}+\zeta\xi_M+1]-\ln(\zeta+\xi_M)\}\\ &-\frac{\xi_N}{\xi_M+\xi_N}\frac{C_1}{(1-\xi_N^2)^{1/2}}\{\ln[(1-\xi_N^2)^{1/2}(1-\zeta^2)^{1/2}-\zeta\xi_N+1]-\ln(\zeta-\xi_N)\}+C_2.\end{aligned} \tag{3.16}$$

The mapping of the point E gives

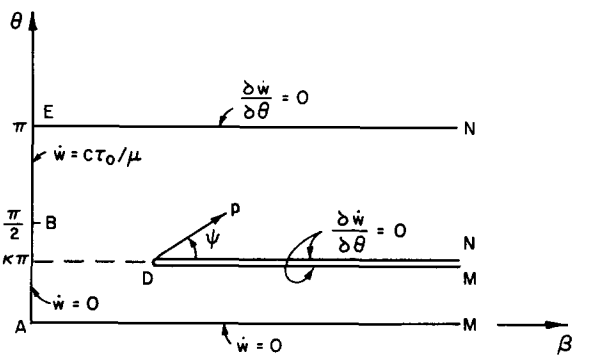

Fig. 4. Domain in the $\theta - \beta$ plane.

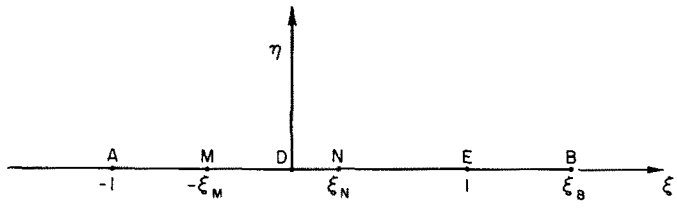

Fig. 5. Mapping on the $\zeta = \xi + i\eta$ plane.

$$C_2 = i\pi. \tag{3.17}$$

Considering the change in imaginary parts at M and N we obtain

$$\kappa = -C_1\xi_M/(\xi_M + \xi_N)(1-\xi_M^2)^{1/2} \tag{3.18}$$

$$1-\kappa = -C_1\xi_N/(\xi_M + \xi_N)(1-\xi_N^2)^{1/2} \tag{3.19}$$

respectively. Eliminating C_1 from eqns (3.18) and (3.19), and substituting the results in eqn (3.16) we find

$$\begin{aligned}\omega(\zeta) = {} & \kappa\{\ln[(1-\xi_M^2)^{1/2}(1-\zeta^2)^{1/2} + \zeta\xi_M + 1] - \ln(\zeta + \xi_M)\} \\ & + (1-\kappa)\{\ln[(1-\xi_N^2)^{1/2}(1-\zeta^2)^{1/2} - \zeta\xi_N + 1] - \ln(\zeta - \xi_N)\} + i\pi.\end{aligned} \tag{3.20}$$

A comparison of the coordinates of point D in the γ- and ζ-planes, results in the relation

$$\ln\left[\frac{c}{v} + \left(\frac{c^2}{v^2} - 1\right)^{1/2}\right] + i\kappa\pi = \omega(0). \tag{3.21}$$

The mapping of the point B yields

$$-\kappa\cos^{-1}\frac{1+\xi_B\xi_M}{\xi_B+\xi_M} + (1-\kappa)\cos^{-1}\frac{\xi_B\xi_N - 1}{\xi_B - \xi_N} = \frac{\pi}{2} - \kappa\pi. \tag{3.22}$$

For given values of κ and v/c, ξ_M and ξ_N can now be computed from eqns (3.18), (3.19) and (3.21), while ξ_B can subsequently be computed from eqn (3.22). These computations must be carried out on a digital computer. The values for limiting cases can, however, be obtained analytically, as

$$\kappa = 0: \quad \xi_M = 0; \quad \xi_N = v/c; \quad \xi_B = c/v \tag{3.23}$$

$$\kappa = 0{\cdot}5: \quad \xi_M = v/c; \quad \xi_N = v/c; \quad \xi_B \to \infty \tag{3.24}$$

$$\frac{v}{c} \ll 1: \quad \xi_M = \left(\frac{\kappa}{1-\kappa}\right)^{1-\kappa}\frac{v}{c}; \quad \xi_N = \left(\frac{\kappa}{1-\kappa}\right)^{-\kappa}\frac{v}{c}; \quad \xi_B = \frac{\kappa^\kappa(1-\kappa)^{1-\kappa}}{1-2\kappa}\frac{c}{v}. \tag{3.25}$$

This completes the computation of the pertinent points in the ζ-plane.

The boundary conditions shown in Fig. 4 transform into the following conditions on the real axis in the ζ-plane.

$$-\infty < \xi \leq -\xi_M: \quad \dot{w} = 0 \tag{3.26}$$

$$-\xi_M < \xi < 1: \quad \partial\dot{w}/\partial\eta = 0 \tag{3.27}$$

$$1 < \xi < \xi_B: \quad \dot{w} = c\tau_0/\mu \tag{3.28}$$

$$\xi_B \leq \xi < \infty: \quad \dot{w} = 0. \tag{3.29}$$

Denoting

$$\dot{w} = Re\, F(\zeta), \tag{3.30}$$

the analytic function $F(\zeta)$ can be obtained analogously to the solution of similar problems in [13] and [18]. From eqn (3.27) it is noted that $F'(\zeta)$, where the prime denotes differentiation with respect to the argument, is real in the interval $-\xi_M < \xi < 1$, while $F'(\zeta)$ is imaginary along the remaining portion of the real axis. The discontinuity in $\dot{w}$ at $\xi = \xi_B$ suggests a simple pole at that point. The following expression satisfies these conditions:

$$F'(\zeta) = \frac{iA}{\zeta - \xi_B} \frac{(\xi_B - 1)^{1/2}(\xi_B + \xi_M)^{1/2}}{(\zeta - 1)^{1/2}(\zeta + \xi_M)^{1/2}} \tag{3.31}$$

where A is a real-valued constant. Integrating with respect to ζ and applying the condition at $\zeta = \xi_B$ we find

$$\dot{w} = A\, Im \ln \frac{F(\zeta)}{(\zeta - \xi_B)T} \tag{3.32}$$

where

$$A = c\tau_0/\mu\pi, \tag{3.33}$$

and

$$F(\zeta) = [(\zeta + \xi_M)^{1/2}(\xi_B - 1)^{1/2} + (\zeta - 1)^{1/2}(\xi_B + \xi_M)^{1/2}]^2 \tag{3.34}$$

$$T = [(\xi_B - 1)^{1/2} + (\xi_B + \xi_M)^{1/2}]^2. \tag{3.35}$$

It can be verified that $\dot{w}$ as given by eqn (3.32) does indeed satisfy the boundary conditions (2.26)–(3.29).

To obtain an explicit expression for $\dot{w}$ as a function of r/t and θ, ζ has to be solved in terms of γ from the mapping function $\gamma = \omega(\zeta)$ given by eqn (3.20). This appears to be rather difficult. Without inverting the mapping function it is, however, possible to derive explicit expressions for the singular parts of the stresses and the particle velocity in the vicinity of the moving crack tip.

In the $\theta - \beta$ plane shown in Fig. 4, we consider a cylindrical coordinate system z, p, ψ centered at D. In the strip $\dot{w}$ is governed by Laplace's equation, and $\partial\dot{w}/\partial\theta$ vanishes on the surfaces of the slit. This implies that $\partial\dot{w}/\partial p$ and $(1/p)\partial\dot{w}/\partial\psi$, or $\dot{\tau}_{pz}$ and $\dot{\tau}_{\psi z}$, show square root singularities at the tip of the slit. The forms of $\dot{\tau}_{pz}$ and $\dot{\tau}_{\psi z}$ follow, for example, from the results of [4] as

$$\dot{\tau}_{pz} - i\dot{\tau}_{\psi z} \sim [K/(2p)^{1/2}] \exp(i\psi/2). \tag{3.36}$$

It is not difficult to show that the intensity factor K can be expressed as

$$K = \mu\sqrt{2} \lim_{\zeta \to \xi_D} \frac{[\omega(\zeta) - \omega(\xi_D)]^{1/2} F'(\zeta)}{\omega'(\zeta)}. \tag{3.37}$$

For details we refer to [4] and [13]. In general the function $dF/d\zeta$ is continuous at $\zeta = \xi_D$, and $d\omega/d\zeta$ vanishes as ζ approaches ξ_D. In that case we use the expansions

$$\omega(\zeta) - \omega(\xi_D) = \frac{1}{2}\zeta^2\omega''(\xi_D) + \cdots \tag{3.38}$$

$$\omega'(\xi_D) = \zeta\omega''(\xi_D) + \cdots. \tag{3.39}$$

In the limit eqn (3.37) then yields

$$K = \mu F'(\xi_D)/[\omega''(\xi_D)]^{1/2}. \tag{3.40}$$

For the problem at hand we find by using eqns (3.15) and (3.31)

$$K = -\frac{c\tau_0}{\pi} \frac{\xi_N(\xi_B - 1)^{1/2}(\xi_B + \xi_M)^{1/2}}{(1 - \kappa)^{1/2}\xi_B(\xi_M + \xi_N)^{1/2}(1 - \xi_N^2)^{1/4}}. \tag{3.41}$$

The factor K is plotted in Fig. 6.

The intensity factor K refers to fields in the $\beta - \theta$ plane. We still have to find the shear stresses in the vicinity of the crack tip in the physical plane, i.e. in terms of the polar coordinates R and φ shown in Fig. 2. After a number of manipulations, which are described in some detail in [13] we obtain

$$\tau_{\varphi z} \sim k_\tau \Phi_\tau\left(\frac{v}{c}, \varphi\right) \Big/ R^{1/2} \tag{3.42}$$

where

$$k_\tau = \left(1 - \frac{v^2}{c^2}\right)^{1/4} \left(\frac{t}{v}\right)^{1/2} K \tag{3.43}$$

and Φ_τ is defined by eqn (2.15). It is, of course, not surprising that the function Φ_τ appears in this result, since it was shown in [12] that the angular variation of the near tip stress field depends only on the instantaneous value of the speed of crack propagation.

In an analogous manner we can find

$$\dot{w} = k_w \Phi_1\left(\frac{v}{c}, \varphi\right) \Big/ R^{1/2}, \tag{3.44}$$

where

$$k_w = \left(1 - \frac{v^2}{c^2}\right)^{-1/4} (vt)^{1/2} \frac{1}{\mu} K. \tag{3.45}$$

In the range $0 \leq \varphi \leq \pi$ the function $\Phi_1\ (v/c, \varphi)$ is given by eqn (2.16).

The limitcase $\kappa \to 0$ requires some special attention. By employing the results stated in eqn (3.23) in the expression for K given by eqn (3.41) we find in the limit $\kappa \to 0$

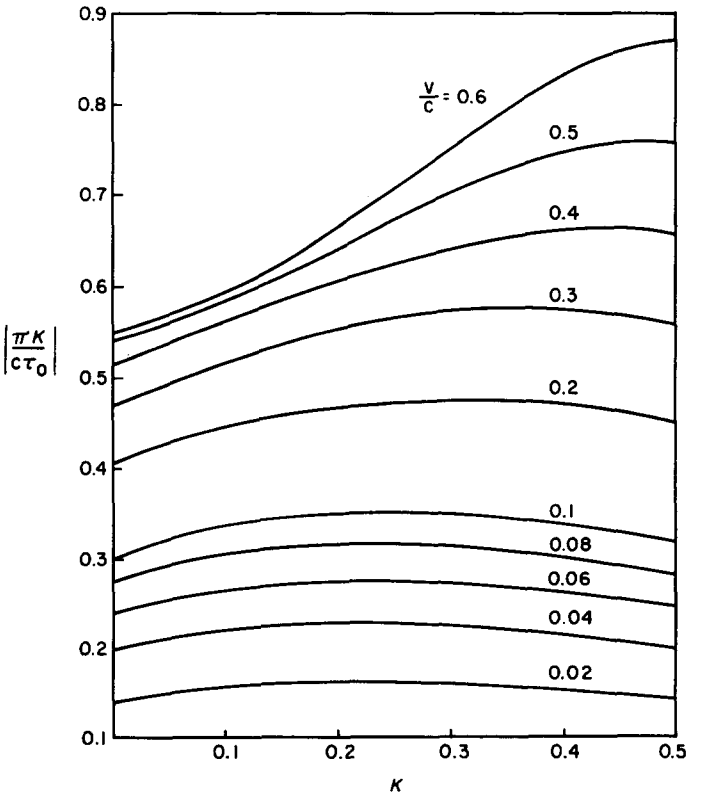

Fig. 6. Factor K vs κ for various values of v/c.

$$K = -\frac{c\tau_0}{\pi}\frac{(1-v/c)^{1/4}}{(1+v/c)^{1/4}}\left(\frac{v}{c}\right)^{1/2}. \tag{3.46}$$

Equation (3.46) may be compared with the corresponding K for the case that the crack does not bifurcate, but propagates in its own plane. By examining the geometry of the mapping it is not difficult to see that the point M then coincides with the point D, while the positions of N and B are given by eqn (3.23). The corresponding expressions for $F'(\zeta)$ and $\omega'(\zeta)$ follow from eqns (3.31) and (3.15) as

$$F'(\zeta) = \frac{c\tau_0}{\mu\pi}\frac{i}{\zeta - c/v}\frac{(c/v-1)^{1/2}(c/v)^{1/2}}{(\zeta-1)^{1/2}\zeta^{1/2}} \tag{3.47}$$

$$\omega'(\zeta) = \frac{C_1}{(\zeta - v/c)(1-\zeta^2)^{1/2}}, \tag{3.48}$$

where C_1 follows from eqns (3.19) as

$$C_1 = -(1-v^2/c^2)^{1/2}. \tag{3.49}$$

The factor K now follows directly from eqn (3.37) as

$$K = -\frac{c\tau_0}{\pi}\frac{(1-v/c)^{1/4}}{(1+v/c)^{1/4}}\left(\frac{v}{c}\right)^{1/2}\sqrt{2}. \tag{3.50}$$

The difference between eqns (3.46) and (3.50) is in the multiplying factor $\sqrt{2}$. Thus, when the crack bifurcates with infinitesimally small angle, the intensity factors drop considerably. For the quasistatic case it was found by Smith [Ref. 5, eqns (28) and (31)] that for small bifurcation angles the critical stress is $\sqrt{2}$ times as large as for propagation along a single segment in the plane of the crack, which is consistent with the results found here. For the present analysis the difference between eqns (3.46) and (3.50) does, however, *not* imply that bifurcation is unlikely to occur, as we shall see in the next section.

For various values of v/c the factor K given by eqn (3.41) is plotted in Fig. 6. It is noted that the maximum of K shifts to a higher value of κ as v/c increases.

4. BIFURCATION OF A RUNNING CRACK

The results obtained in Sections 2 and 3 can now be used to analyze the conditions for bifurcation of a running crack. It was pointed out in Section 2 that for a running crack which bifurcates at time $t = t_{bf}$, the stresses which must be removed from the crack branches are given by eqn (2.19), where $R < vt$, and $\varphi = \pi \pm \kappa\pi$.

Let us suppose that upon bifurcation of the running crack the stress distribution near the branch tip D is of the general form

$$\tau^*_{\varphi z} \sim k^*_\tau(\bar{t})\Phi_\tau\left(\frac{v}{c}, \bar{\varphi}\right)\Big/\bar{R}^{1/2} \tag{4.1}$$

where

$$\bar{t} = t - t_{bf}, \tag{4.2}$$

and $\bar{\varphi}$ and $\bar{R}$ are defined in Fig. 2. In the previous section we have found that the near tip stress field for instantaneous bifurcation upon the application of equal and opposite uniform antiplane shear tractions to the two semi-infinite surfaces of a stationary crack, is defined by eqn (3.42). If for that case the crack does not bifurcate, nor propagate in its own plane, the near tip stress field is

$$\tau_{\theta z} = Bt^{1/2}H(t)\cos(\tfrac{1}{2}\theta)/r^{1/2} \tag{4.3}$$

where

$$B = \frac{2}{\pi} c^{1/2} \tau_0. \tag{4.4}$$

This result follows from eqn (9.96) of [17], by setting $\alpha = \pi/2$. Clearly, the result (3.42) can also be regarded as being a consequence of removing stresses of the form (4.3) from the crack branches. Thus, we now have a known stress (3.42) due to the removal of a known distribution of surfaction tractions (4.3), and an unknown stress (4.1) due to the removal of the known distribution (2.19). Apart from constants the difference between eqn (2.19) and (4.3) is, however, only in the time dependence; eqn (2.19) contains a step time dependence, while in eqn (4.3) the dependence on time is as $t^{1/2}$. These results then suggest that at least for very small times, $k_\tau^*(t)$ and $k_\tau(t)$ are related by superposition considerations as

$$k_\tau(t) = \frac{B}{A} \int_0^t k_\tau^*(t-s) \mathrm{d}(s^{1/2}). \tag{4.5}$$

This equation can easily be solved for k_τ^* as

$$k_\tau^* = \frac{1}{(2a)^{1/2}} \left(\frac{c}{v}\right)^{1/2} \left(1 - \frac{v^2}{c^2}\right)^{1/4} \frac{K}{c\tau_0} S(t_{bf}). \tag{4.6}$$

In a similar manner we can obtain

$$k_w^* = \frac{1}{\mu} \frac{(vc)^{1/2}}{(2a)^{1/2}} \left(1 - \frac{v^2}{c^2}\right)^{-1/4} \frac{K}{c\tau_0} S(t_{bf}). \tag{4.7}$$

The corresponding flux of energy into a crack tip is

$$F^* = \frac{\pi}{\mu} \frac{c}{a} \left(\frac{K}{c\tau_0}\right)^2 [S(t_{bf})]^2. \tag{4.8}$$

The conditions are right for crack bifurcation at time $t = t_{bf}$ with velocity v, if the balance of rates of energies (2.6) can be satisfied, which implies

$$\left(\frac{\pi K}{c\tau_0}\right)^2 = \frac{2\pi a \gamma_F \mu}{[S(t_{bf})]^2} \frac{v}{c}. \tag{4.9}$$

The left hand side of eqn (4.9) can immediately be obtained from the results plotted in Fig. 6. Since eqn (4.9) contains two unknowns, namely v and κ, an additional condition is required. Such an additional condition is that only a point where F^* is a maximum with respect to κ defines a case of stable crack propagation relative to variations of κ. Thus in Fig. 7 the maxima of $(\pi K/c\tau_0)^2$ with respect to κ have been replotted versus v/c.

In Fig. 7, we have also plotted the curve $2(1-\alpha)^{1/2}\alpha/(1+\alpha)^{1/2}$ for propagation in the plane of the crack, and the line $2\pi a\gamma_F\mu\alpha/[S(t)]^2$. The slope of the line decreases as $S(t)$ increases. When $S(t) = S_{cr} = (\pi\mu\gamma_F a)^{1/2}$ the necessary condition for fracture is met. The load $S(t)$ may exceed S_{cr} before fracture in the plane of the crack may actually start. If that is the case there is an instantaneous speed of crack propagation, and subsequent values of $\mathrm{d}X/\mathrm{d}t$ as $S(t)$ increases can be determined as the intersection of the line and the curve, as previously discussed in Section 2. From Fig. 7 we note, however, that as $S(t)$ increases, the line $2\pi a\gamma_F\mu\alpha/[S(t)]^2$ will eventually touch the curve for $(\pi K/c\tau_0)^2_{\max}$ which is also plotted in Fig. 7. When that takes place eqn (4.9) is satisfied, and the necessary condition for crack bifurcation is satisfied. Since both the curves $2(1-\alpha)^{1/2}\alpha/(1+\alpha)^{1/2}$ and $(\pi K/c\tau_0)^2_{\max}$ are independent of the load, it is evident that the pertinent parameter governing initiation of crack bifurcation is the speed $\mathrm{d}X/\mathrm{d}t$ of the crack in its own plane. The speed follows from the intersection of $2(1-\alpha)^{1/2}\alpha/(1+\alpha)^{1/2}$ with the straight line through the origin which touches the curve $(\pi K/c\tau_0)^2_{\max}$. We find

$$\left(\frac{1}{c}\frac{\mathrm{d}X}{\mathrm{d}t}\right)_{\text{bifurcation}} \sim 0{\cdot}375. \tag{4.10}$$

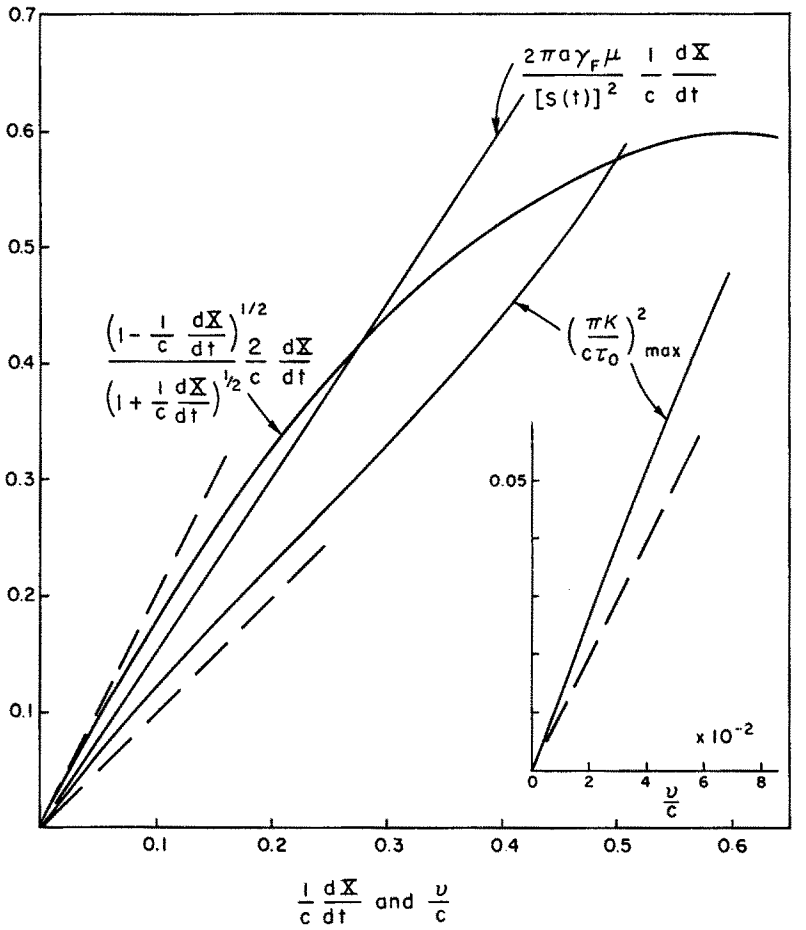

Fig. 7. Terms appearing in the balances of rates of energies for propagation in the plane of the crack and for symmetric bifurcation.

The insert in Fig. 7 shows a somewhat enlarged view of the region for small v/c. The speed of bifurcation is found as

$$\left(\frac{v}{c}\right)_{\text{bifurcation}} \sim 0{\cdot}02. \tag{4.11}$$

The angle of bifurcation is

$$\kappa\pi \sim 0{\cdot}22\pi. \tag{4.12}$$

Equation (4.10) indicates of course only the velocity of in-plane crack propagation at which the necessary condition for bifurcation is first met. Equations (4.11) and (4.12) indicate the corresponding speed and angle of bifurcation. Note that the speed of bifurcation is much smaller than the preceding in-plane crack propagation velocity. Once bifurcation has started the curve for propagation in the plane of the crack becomes, however, again operative, and the speed of crack propagation can increase rapidly until the conditions is met for another bifurcation, as the load is increased.

5. CONCLUDING REMARKS

Solutions of antiplane (Mode-III) problems frequently suggest the proper steps for the attack on inplane problems. There are, however, some principal differences in the basic mechanisms of crack bifurcation for the antiplane and inplane cases, and these should be kept in mind. Branches of a primary crack under pure mode-I loading generally are subjected to both Mode-I and

Mode-II loading conditions. Mixed loading conditions do not occur for crack bifurcation in antiplane strain.

The experimental information available in the literature is for the inplane case. In addition to the dynamic studies presented in [1–3], experimental results were also reported in [19–22]. There are several differences between the experimental results for the inplane case and the analytical results for the antiplane case obtained in this paper. In eqn (4.12) the angle of bifurcation is stated as approximately 40°. Experimentally the following angles were found for the inplane case: Congleton [19]: ~20°; Clark, Irwin [20]: ~17°; Kalthof [3]: ~15°; Kobayashi *et al.* [21]: ~13°. In the present paper the post-bifurcation speed was computed as $v/c \approx 0{\cdot}02$, see eqn (4.11). Döll [22] measured the speed of the bifurcating branches as approximately 90% of the speed of the primary crack tip just prior to bifurcation. Kobayashi *et al.* [21] found slightly smaller values. In the present paper the speed at which bifurcation of the primary crack tip occurs was obtained as 0·375 times the speed of transverse waves, see eqn (4.10). For the inplane case Kerkhof [2] measured a maximum crack velocity of approximately one third of the speed of longitudinal waves.

The differences between the analytical results for the antiplane case presented in this paper and the experimental results for the inplane case cited above can primarily be ascribed to differences in the basic fracture mechanisms. Another reason for the differences could be that in the analysis γ_F (the apparent surface energy) was assumed independent of the crack tip velocity. It has, however, been reported that experiments on steel under Mode-I loading show that for a rapidly propagating crack tip the apparent surface energy may be more than a factor of ten higher than for slowly propagating crack tips. In principle it would not be difficult to extend the analysis of this paper to the case that γ_F depends on the crack propagation velocity, but this would require an explicit expression for γ_F in terms of the crack propagation velocity. Such an expression is presently not available.

Acknowledgements—This work was carried out in the course of research sponsored by the Office of Naval Research under Contract ONR N00014-67-A-0356-0034 with Northwestern University. The author should like to acknowledge the assistance of Dr. V. K. Varatharajulu in some phases of this work.

REFERENCES

1. H. Schardin, Velocity effects in fracture, In *Fracture* (Edited by B. L. Averbach, D. K. Felbeck, G. T. Hahn and D. A. Thomas), pp. 297–330. Wiley, New York (1959).
2. F. Kerkhof, *Bruchvorgänge in Gläsern*. Verlag der Deutschen Glastechnischen Gesellschaft, Frankfurt (Main), (1970).
3. J. F. Kalthof, On the propagation direction of bifurcated cracks, In *Dynamic Crack Propagation* (Edited by G. C. Sih), pp. 449–458. Noordhoff, Leyden (1974).
4. G. C. Sih, Stress distribution near internal crack tips for longitudinal shear problems, *J. Appl. Mech.* **32**, 51 (1965).
5. E. Smith, Crack bifurcation in brittle solids, *J. Mech. Phys. Solids* **16**, 329 (1968).
6. M. A. Hussain, S. L. Pu and J. Underwood, Strain energy release rate for a crack under combined Mode I and Mode II, Report of Benet Weapons Laboratory, Watervliet Arsenal, Watervliet, New York (1973).
7. K. Palaniswamy and W. G. Knauss, On the problem of crack extension in brittle solids under general loading, Graduate Aeronautical Laboratories, California Institute of Technology, Report SM 74-8 (1974).
8. G. C. Sih, A special theory of crack propagation, In *Methods of analysis and solutions of crack problems*. (Edited by G. C. Sih). Noordhoff, Leyden (1972).
9. E. H. Yoffe, The moving Griffith crack, *Philosophical Magazine* **42**, 739 (1951).
10. F. Nilsson, A note on the stress singularity at a non-uniformly moving crack tip. *J. Elasticity* **4**, 73 (1974).
11. L. B. Freund and R. Clifton, On the uniqueness of plane elastodynamic solutions for running cracks. *J. Elasticity* **4**, 293 (1974).
12. J. D. Achenbach and Z. P. Bažant, Elastodynamic near-tip stress and displacement fields for rapidly propagating cracks in orthotropic materials. *J. Appl. Mech.* **42**, 183 (1975).
13. J. D. Achenbach and V. K. Varatharajulu, Skew crack propagation at the diffraction of a transient stress wave. *Quart. Appl. Math.* **XXXII**, 123 (1974).
14. J. D. Achenbach, Dynamic effects in brittle fracture. In *Mechanics Today* (Edited by S. Nemat-Nasser), Vol. I, pp. 1–57, Pergamon, New York (1974).
15. L. B. Freund, Energy flux into the tip of an extending crack in an elastic solid. *J. Elasticity* **2**, 341 (1972).
16. M. Williams, Stress singularities resulting from various boundary conditions in angular corners in extension. *J. Appl. Mech.* **19**, 526 (1952).
17. J. D. Achenbach, *Wave Propagation in Elastic Solids*. North-Holland Publ. Co./American Elsevier, Amsterdam/New York (1973).
18. G. C. Sih, Boundary problems for longitudinal shear cracks. In *Developments in Theoretical and Applied Mechanics* (Edited by W. A. Shaw), Vol. 2, pp. 117–130 (1965).
19. J. Congleton, Practical applications of crack-branching measurements. In *Dynamic Crack Propagation* (Edited by G. C. Sih), pp. 427–438. Noordhoff, Leyden (1974).
20. A. B. J. Clark and G. R. Irwin, Crack propagation behaviors. *Experimental Mechanics* **6**, 321 (1966).
21. A. S. Kobayashi, B. G. Wade, W. B. Bradley and S. T. Chiu, Crack branching in Homalite-100 sheets. *Engng. Fract. Mech.* **6**, 81 (1974).
22. W. Döll, Investigations of the crack branching energy, *Int. J. Fract. Mech.* **11**, 184 (1975).